

Pseudophomins A–D Produced from *Pseudomonas* sp. HN8-3 Using an OSMAC Approach and Their Roles in Biocontrol of *Phytophthora capsici* in Cucumbers

Zongwang Ma* and Jun Sheng



Cite This: <https://doi.org/10.1021/acs.jafc.3c00137>



Read Online

ACCESS |

Metrics & More

Article Recommendations

Supporting Information

ABSTRACT: In this study, two new cyclic lipopeptides (CLPs) pseudophomins C (3) and D (4) and two known CLPs pseudophomins A (1) and B (2) were produced and characterized from the bacterial supernatant of *Pseudomonas* sp. HN8-3 by an OSMAC (one strain-many compounds) approach. OSMAC is a strategy that involves feeding of a single microorganism with divergent substrates to stimulate the production of new secondary metabolites. These pseudophomins were purified and identified via chromatographic methods, droplet collapse assay, genome mining, spectroscopic and spectrometric analyses, and single-crystal X-ray diffraction (XRD). Moreover, bioactivity tests showed that pseudophomins could lyse the zoospores of *Phytophthora capsici* in vitro, and coapplication of pseudophomins with zoospores of *P. capsici* further reduced the incidence of *P. capsici* on cucumber leaves. Collectively, these results indicated that pseudophomins have the potential to be developed as biopesticides for controlling *P. capsici* in cucumber.

KEYWORDS: *Pseudomonas* species, pseudophomins, structural characterization, *Phytophthora capsici*, biocontrol

INTRODUCTION

Phytophthora capsici, a destructive oomycete pathogen, is the causal agent of a broad host of vegetables (such as cucurbits, pepper, and tomato).¹ During asexual reproduction, zoospores released from sporangia of this pathogen are the key virulent parts in plants. Attachment and subsequently germination of zoospores on the surface of plant tissues commence an initial stage of the disease cycle of *P. capsici*, finally resulting in sporulation on plant tissues when this pathogen switches from biotrophic to necrotrophic stages.² The epidemic of *P. capsici* is a great threat to the production and postharvest storage of corresponding vegetables.

Biocontrol of phytopathogens by plant-associated bacteria has been intensively studied for decades. *Pseudomonas* spp. are one of the well-studied biocontrol bacteria, and they are even the main ingredients of some commercialized biopesticides.^{3,4} From a taxonomic perspective, more than 300 types of strains of *Pseudomonas* species have been characterized to date.⁵ Importantly, *Pseudomonas* species can synthesize versatile secondary metabolites with broad spectra of bioactivities, among which antagonistic properties against phytopathogens and triggering of plant innate immunity are of utmost interest for biocontrol.^{4,6,7}

Plant-associated *Pseudomonas* species can secrete biocontrol-related biosurfactant CLPs.^{4,8} A molecule of CLP produced by *Pseudomonas* spp. is a nonribosomal peptide synthetase (NRPS)-derived natural product with a peptidic sequence linked to a saturated (or unsaturated) fatty acid moiety.⁹ Specific biosynthetic gene clusters (BGCs) can encode NRPSs in *Pseudomonas* spp. Moreover, different modules in NRPSs are responsible for peptide biosynthesis. There are generally adenylation (A), condensation (C), and thiolation (T)

domains in each module, and the terminal thioesterase (Te) domains in NRPSs have ceased the biosynthesis of CLPs.¹⁰ The BGC coding for NRPS of CLPs can be easily detected from the genome of the strain producing them by antiSMASH.¹¹ BGCs coding for NRPSs of CLP orfamide, bananamide, pseudodesmin, viscosinamide, putisolvin, and medipeptin have been successfully identified by this technique from genomes of the *Pseudomonas* strains producing them.^{6,12–15} In addition, phylogenetic analyses of adenylation (A) and condensation (C) domains of NRPSs will tentatively establish the possible composition and stereochemistry for amino acids in these CLPs, which could be useful for further identification of corresponding CLPs. Therefore, genome mining and analyses of NRPSs have been successfully applied for the discovery of CLPs derived from *Pseudomonas* spp. in recent years. A previous study has shown that the CLP putisolvin produced by *Pseudomonas* species displayed potent biocontrol activities in decreasing the incidence of *P. capsici* in plants.¹⁶ However, the biocontrol capacities of other CLPs produced by *Pseudomonas* spp. against *P. capsici* remain unclear so far and need to be elucidated.

It is reported that the rhizosphere soil consists of a high abundance of *Pseudomonas* species.^{8,17} *Pseudomonas* sp. HN8-3 was isolated from the rhizosphere soil of the *Lens culinaris*

Received: January 8, 2023

Revised: March 29, 2023

Accepted: April 6, 2023

Table 1. ^1H and ^{13}C NMR Data (DMF- d_7) of 1 and 2^a

moiety	position	1		2		moiety	position	1		2	
		δ_{C}	δ_{H} (J in Hz)	δ_{C}	δ_{H} (J in Hz)			δ_{C}	δ_{H} (J in Hz)	δ_{C}	δ_{H} (J in Hz)
Leu ₁	CO	175.2		175.2		Leu ₇	CO	171.0		171.0	
	NH		9.08d (4.4)		9.07d (4.9)		NH		7.16d (7.1)		7.16d (7.2)
	α -C	52.8	4.15m	52.8	4.15m		α -C	53.0	4.28m	53.0	4.28m
	β -C	39.1	1.74m	39.1	1.74m		β -C	41.0	1.67m; 1.92m	41.0	1.67m; 1.92m
	γ -C	24.3	1.93m	24.3	1.93m		γ -C	24.4	1.84m	24.4	1.84m
	δ_1 -C	20.4 ^a	0.89m ^b	20.4 ^a	0.89m ^b		δ_1 -C	22.7 ^a	0.89m ^b	22.7 ^a	0.89m ^b
Glu ₂	δ_2 -C	20.6 ^a	0.96m ^b	20.6 ^a	0.96m ^b	δ_2 -C	23.0 ^a	0.98m ^b	23.0 ^a	0.98m ^b	
	CO	173.7		173.7		Ser ₈	CO	172.7		172.7	
	NH		9.25d (2.0)		9.22d (3.2)		NH		8.04d (8.3)		8.04d (8.3)
	α -C	56.3	4.14m	56.3	4.14m		α -C	56.5	4.42n	56.5	4.42n
	β -C	26.2	2.12m	26.2	2.12m		β -C	62.0	3.71dd (3.5; 3.7); 3.93m	62.0	3.71dd (3.7; 3.8); 3.93m
	γ -C	30.6	2.54m	30.6	2.54m		Ile ₉	CO	169.2		169.2
δ -CO	174.2		174.2		NH				6.96d (9.8)		6.96d (9.8)
Thr ₃	CO	175.5		175.5		α -C		56.2	4.60dd (3.1; 3.1)	56.2	4.60dd (3.1; 3.1)
	NH		8.40d (6.7)		8.40d (6.8)	β -C		36.4	1.97m	36.4	1.97m
	α -C	60.5	4.26m	60.5	4.26m	γ -C		24.5	1.26m	24.5	1.26m
	β -C	69.3	5.46s	69.3	5.46s	δ_1 -C		16.2	1.01t (6.0)	16.2	1.01m
	γ -C	17.7	1.37d (6.0)	17.7	1.37d (6.1)	δ_2 -C	11.6	0.89m	11.6	0.89m	
	δ -CO	174.2		174.2		Fatty acid	CO	170.8		170.8	
Ile ₄	CO	173.6		173.6			CH ₂ α	43.9	2.51m	43.9	2.51m
	NH		7.61d (6.5)		7.60d (6.5)		CH β	68.6	4.08m	68.6	4.08m
	α -C	62.0	3.76m	62.0	3.76m		CH ₂ γ	37.6	1.51m	37.6	1.51m
	β -C	34.8	2.14m	34.8	2.14m		CH ₂ δ	25.6	1.37m; 1.49m	25.6	1.37m; 1.49m
	γ -C	25.5	1.22m	25.5	1.22m		CH ₂ e	29.5	1.28m	29.5	1.28brs
	δ_1 -C	15.4	0.85m	15.4	0.85m		CH ₂ η	29.5	1.28m	29.5	1.28brs
Leu ₅	δ_2 -C	10.1	0.93m	10.1	0.93m		CH ₂ θ	31.7	1.26m	29.5	1.28brs
	CO	173.0		173.0			CH ₂ i	22.5	1.29m	29.5	1.28brs
	NH		7.68d (4.6)		7.66d (4.8)		CH ₂ /CH ₃ κ	13.7	0.89t	31.7	1.26m
	α -C	54.4	4.10m	54.4	4.10m		CH ₂ λ			22.5	1.28brs
	β -C	39.6	1.52m; 1.80m	39.6	1.52m; 1.80m		CH ₃ μ			13.7	0.89t
	γ -C	24.6	1.72m	24.6	1.72m	Ser ₆	CO	172.9		172.9	
δ_1 -C	22.7 ^a	0.89m ^b	22.7 ^a	0.89m ^b	NH			7.54d (7.6)		7.54d (7.6)	
δ_2 -C	22.5 ^a	0.87m ^b	22.5 ^a	0.87m ^b	α -C		56.4	4.34n	56.4	4.34n	
Ser ₆	CO	172.9		172.9			β -C	62.9	3.89dd (2.6; 2.6); 4.13m	62.9	3.89dd (2.8; 3.3); 4.13m
	NH		7.54d (7.6)		7.54d (7.6)						
	α -C	56.4	4.34n	56.4	4.34n						
	β -C	62.9	3.89dd (2.6; 2.6); 4.13m	62.9	3.89dd (2.8; 3.3); 4.13m						

^a or ^b presents that NMR data may be interchangeable within the column of the same superscript.

Medic. plants in this study. CLPs produced by *Pseudomonas* sp. HN8-3 were purified and characterized via multiple techniques. The antifungal activity of these CLPs against *P. capsici* was evaluated further in vitro and on cucumber leaves.

MATERIALS AND METHODS

General Experimental Procedures. A flash column (50 × 80 mm) loading of 5 g of YMC ODS-A gel (50 μm , YMC Co., Ltd., Japan) was used for solid-phase extraction (SPE). The HPLC analysis was carried out on Agilent 1100 series (Agilent Technologies) equipped with a YMC ODS-A column (150 × 4.6 mm, 5 μm) for analytical purposes and with a YMC ODS-A column (250 × 10 mm, 5 μm) for semipreparative purpose. High-resolution mass spectrometry (HR-MS) data were collected on a matrix-assisted laser desorption/ionization (MALDI) time-of-flight (TOF) mass spectrometer (Bruker MALDI-TOF Autoflex III, Bruker Corporation). Melting point (mp) was acquired on a melting point meter (JHX-SPLUS, Shanghai Jiahang Instrument Co., Ltd, China). UV absorbance was measured on a UV spectrophotometer (Jasco, Jasco Corporation, Japan). Optical rotation was recorded on a P-2200 polarimeter (Jasco, Jasco Corporation, Japan). Infrared spectroscopy (IR) was performed on a

Jasco ATR MIRacle spectrophotometer (Jasco Corporation, Japan). 1D and 2D nuclear magnetic resonance (NMR) data were acquired on an NMR spectrometer (Agilent DD2-600 MHz, Agilent Technologies). *N,N*-Dimethylformamide- d_7 (DMF- d_7 , Cambridge Isotope Laboratories, Inc., USA) containing 0.03% (*v/v*) tetramethylsilane was used for NMR measurements. An XtaLAB AFC12 (RINC); Kappa single diffractometer was used for single-crystal XRD. Plants were routinely cultivated in a growth chamber (photoperiod with 12 h light/12 h dark, 25 °C, HPG-280BX, HDL Apparatus, China). A light microscope (BXJ903, Shanghai Qibu Biological Technology Co. Ltd, China) was used for the observation of zoospores.

Isolation of Biosurfactant-Producing Microorganisms. 0.5 g of rhizosphere soil collected from the *L. culinaris* Medic. plants (Gansu province, China) was well homogenized in 1 mL of sterilized 0.85% (*w/v*) saline solution, and then the solution was diluted to several dilutions by a 10-fold serial dilution. 100 μL of diluted sample was plated on King's medium B (KB, 20 g of protease peptone D, 1.5 g of K_2HPO_4 , 1.5 g of MgSO_4 , 10 mL of glycerol, per liter) agar, and the plates were incubated at 28 °C for 2 days until single colonies formed. The plates were further studied for the production of green fluorescence under UV light. The bacterial colonies showing green

Table 2. ^1H and ^{13}C NMR Data (DMF- d_7) of 3 and 4^a

moiety	position	3		4		moiety	position	3		4		
		δ_{C}	δ_{H} (J in Hz)	δ_{C}	δ_{H} (J in Hz)			δ_{C}	δ_{H} (J in Hz)	δ_{C}	δ_{H} (J in Hz)	
Leu ₁	CO	174.1		174.1		Leu ₇	CO	171.2		171.2		
	NH		8.95s		8.97d (4.4)		NH		7.05d (7.6)		7.05d (7.6)	
	α -C	53.5	4.15m	53.5	4.15m		α -C	53.0	4.29m	53.0	4.29m	
	β -C	39.6	1.73m	39.6	1.73m		β -C	41.0	1.84m	41.0	1.84m	
	γ -C	24.4	1.87m	24.4	1.87m		γ -C	24.9	1.66m	24.9	1.66m	
	δ_1 -C	21.5 ^a	0.89m ^b	21.5 ^a	0.89m ^b		δ_1 -C	22.6 ^a	0.98m ^b	22.6 ^a	0.98m ^b	
Glu ₂	δ_2 -C	22.2 ^a	0.92m ^b	22.2 ^a	0.92m ^b	δ_2 -C	20.8 ^a	0.86m ^b	20.8 ^a	0.86m ^b		
	CO	174.0		174.0		Ser ₈	CO	172.8		172.8		
	NH		9.29d (3.5)		9.30d (4.5)		NH		8.06d (10.9)		8.06d (8.1)	
	α -C	55.0	4.11m	55.0	4.11m		α -C	56.6	4.39m	56.6	4.39m	
	β -C	26.3	2.12m	26.3	2.12m		β -C	62.2	3.74m; 3.89m	62.2	3.74m; 3.89m	
	γ -C	30.5	2.57m	30.5	2.57m	Leu ₉	CO	170.6		170.6		
δ -CO	175.8		175.8		NH			7.15d (9.5)		7.14d (9.5)		
CO	175.7		175.7		α -C		49.9	4.61td (3.7; 3.8; 4.1)	49.9	4.61td (3.5; 3.8; 4.2)		
Thr ₃	NH		8.48d (6.4)		8.49d (6.4)	β -C	39.8	1.67m	39.8	1.67m		
	α -C	60.8	4.24m	60.8	4.24m	γ -C	24.6	1.87m	24.6	1.87m		
	β -C	69.4	5.51s	69.4	5.51s	δ_1 -C	21.4 ^a	0.88m ^b	21.4 ^a	0.88m ^b		
	γ -C	18.1	1.38d (5.9)	18.1	1.38d (6.0)	δ_2 -C	23.3 ^a	0.99m ^b	23.3 ^a	0.99m ^b		
	CO	173.1		173.1		Fatty acid	CO	170.8		170.8		
	NH		7.61d (7.5)		7.64d (6.4)		CH ₂ α	43.9	2.51m	43.9	2.51m	
α -C	55.0	4.10m	55.0	4.10m	CH β		68.6	4.08m	68.6	4.08m		
β -C	39.6	1.72m	39.6	1.72m	CH ₂ γ		38.0	1.52m	38.0	1.52m		
γ -C	24.8	1.72m	24.8	1.72m	CH ₂ δ		25.7	1.36m; 1.46m	25.7	1.36m; 1.46m		
δ_1 -C	22.9 ^a	0.90m ^b	22.9 ^a	0.90m ^b	CH ₂ ϵ		29.6	1.28m	29.6	1.28m		
Leu ₄	δ_2 -C	22.8 ^a	0.97m ^b	22.8 ^a	0.97m ^b	CH ₂ η	29.6	1.28m	29.6	1.28m		
	CO	173.8		173.8		CH ₂ θ	32.1	1.27m	29.6	1.28m		
	NH		7.51d (6.0)		7.53d (6.2)	CH ₂ ι	22.9	1.29m	29.6	1.28m		
	α -C	54.2	4.17m	54.2	4.17m	CH ₂ / $\text{CH}_3\kappa$	14.0	0.88t	32.1	1.27m		
	β -C	40.1	1.81m	40.1	1.81m	CH ₂ λ			22.9	1.29m		
	γ -C	24.8	1.75m	24.8	1.75m	CH ₃ μ			14.0	0.88t		
Leu ₅	δ_1 -C	22.8 ^a	0.91m ^b	22.8 ^a	0.91m ^b	Ser ₆	CO	173.8		173.8		
	δ_2 -C	21.0 ^a	0.86m ^b	21.0 ^a	0.86m ^b		NH		7.61d (7.5)		7.61d (7.5)	
	CO	173.8		173.8			α -C	56.6	4.32m	56.6	4.32m	
	NH		7.61d (7.5)		7.61d (7.5)		β -C	63.0	3.89m; 4.11m	63.0	3.89m; 4.11m	
	α -C	56.6	4.32m	56.6	4.32m							
	β -C	63.0	3.89m; 4.11m	63.0	3.89m; 4.11m							

^a or ^b indicates that NMR data may be interchangeable within the column of the same superscript.

fluorescence were selected, streaked, and purified on KB plates. Bacterial cells were collected from KB plates and were suspended in 0.5 mL of KB broth, the solution was homogenized well and was further tested for the production of biosurfactants by the droplet collapse assay.⁸ Testing for the droplet collapse was conducted by dropwise addition of the bacterial solution and KB broth (a negative control) on a hydrophobic surface. A green fluorescence-producing strain HN8-3 was isolated on KB agar, and the droplet collapse assay of the strain was positive.

Genome Sequencing, Genome Mining, and Molecular Phylogeny Analysis. The strain HN8-3 was cultivated on Luria–Bertani (LB, 10 g of tryptone, 5 g of yeast extract, 10 g of NaCl, per liter) agar for 3 days at 28 °C. A single colony was inoculated into a 250 mL flask containing 50 mL of LB broth, and the flask was maintained on a rotary shaker (180 rpm, 28 °C) for 24 h. Bacterial cells were collected by centrifugation at 8000 rpm for 5 min. DNA of the bacterial cells was purified by a DNA isolation kit following the manufacturer's instructions (TaKaRa MiniBEST Bacteria Genomic DNA Extraction Kit Ver.3.0, TaKaRa). The DNA of the bacterial isolate was sequenced on a PacBio platform, and the genome was assembled by Hifiasm software.¹⁸ The genome of *Pseudomonas* sp. HN8-3 has been released in GenBank (accession number: CP086206).

16S rRNA sequences used for phylogeny were either extracted or retrieved from the genome of the bacterial strain or from GenBank. Type strains of the *Pseudomonas fluorescens* subgroup were included in the phylogenetic analysis. 16S rRNA sequences used for phylogeny were aligned by MUSCLE, and the neighbor-joining tree of selected sequences was constructed using MEGA 6.¹⁹ Mining of the BGCs from the genome of the strain HN8-3 was conducted by antiSMASH 6.0.¹¹ Amino acid sequences of adenylation (or condensation) domains from selected NRPSs were extracted from the annotated BGCs of corresponding CLP-producing *Pseudomonas* strains. The amino acid sequences were aligned by MUSCLE, and the neighbor-joining tree of aligned sequences was constructed by MEGA 6.

Liquid Fermentation. KB or the modified KB (MKB) (addition of 5 g of l-Leu in KB broth, per liter) was used for culturing *Pseudomonas* sp. HN8-3. The bacterium was streaked on LB agar and incubated for 3 days at 28 °C. Single colonies were inoculated into several 250 mL flasks containing 50 mL of KB (or MKB) broth. Then, the flasks were incubated on a rotary shaker (180 rpm, 28 °C) for 2 days.

Purification and Compound Identification. The bacterial supernatant was collected by centrifugation (8000 rpm, 5 min) from bacterial cultures. Then, the supernatant was pooled and loaded through an SPE column. The SPE column was sequentially

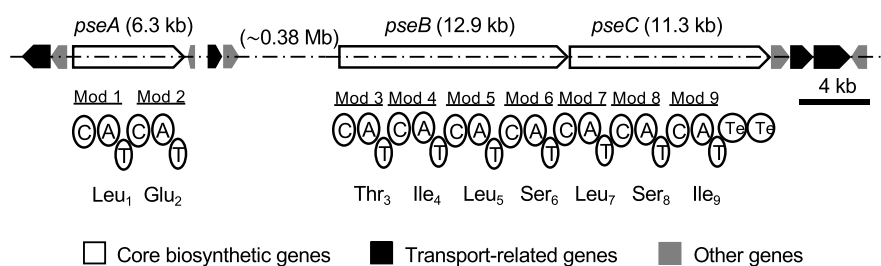


Figure 1. A split NRPS BGC was characterized from *Pseudomonas* sp. HN8-3. There are biosynthesis genes (*pseA*, *pseB*, and *pseC*) in the BGC, and a 0.38 Mb internal distance lies between *pseA* and *pseB*. The module (Mod) for amino acid biosynthesis is composed of A, C, and T domains. The flanking region of the BGC contains transport-related genes and other genes. Scale bar = 4 kb of the nucleotide sequence.

fractionated by 200 mL of 50% MeCN/H₂O (*v/v*) and 200 mL of MeCN, respectively. Then, the fractions obtained from SPE were analyzed by HPLC. The analytical solvent used for HPLC was 85% MeCN/H₂O (*v/v*), with a flow rate of 1.0 mL/min under 210 nm. The fractions from SPE were air-dried as crude extracts, and the crude extracts were dissolved in KB broth at 1 mg/mL. 10 μ L of the solution of crude extracts and 10 μ L of KB broth (a negative control) were carefully added dropwise on a parafilm by a pipette. The positive results from the droplet collapse assay were observed on the MeCN fraction from SPE, indicating that the crude extracts from the fraction contained crude CLPs. 115.6 mg of crude CLPs was yielded from 400 mL of KB cultures, while 459.1 mg of crude CLPs was recovered from 400 mL of MKB cultures using the same protocol as for KB cultures of strain HN8-3.

The semipreparative process by HPLC used 80% MeCN/H₂O (*v/v*) as a solvent, with a flow rate of 2.5 mL/min under 210 nm. The CLP peaks were collected from HPLC, and the fractions were pooled together and then dried, yielding purified compounds. **1** (retention time [*t_R*] = 30.7 min, 30.2 mg) and **2** (*t_R* = 57.6 min, 56.5 mg) were isolated from crude CLPs obtained from the KB supernatant of strain HN 8–3, while **3** (*t_R* = 25.9 min, 26.3 mg) and **4** (*t_R* = 48.0 min, 16.8 mg) were purified from crude CLPs obtained from the MKB supernatant of strain HN8-3.

Pseudophomin A (1): white amorphous powder; mp 217.9 °C; [α]_D²⁵ –12.7 (*c* 0.15, MeOH); IR (KBr) ν_{\max} 3460, 3379, 3294, 2957, 2932, 2874, 1736, 1655, 1539, 1460, 1234, 1076 cm⁻¹; HR-MS *m/z* 1140.7091 [M + H]⁺ (calculated for C₅₅H₉₈N₉O₁₆, 1140.7132, Δ = –3.6 ppm). ¹H and ¹³C NMR data are reported in Table 1.

Pseudophomin B (2): white amorphous powder, mp 246.7 °C; [α]_D²⁵ –16.0 (*c* 0.10, MeOH); IR (KBr) ν_{\max} 3455, 3381, 3287, 2961, 2930, 2874, 1738, 1655, 1535, 1499, 1233, 1076 cm⁻¹; HR-MS *m/z* 1168.7438 [M + H]⁺ (calculated for C₅₇H₁₀₂N₉O₁₆, 1168.7445, Δ = –0.6 ppm). ¹H and ¹³C NMR data are reported in Table 1.

Pseudophomin C (3): white amorphous powder, mp 232.3 °C; [α]_D²⁵ –18.8 (*c* 0.24, MeOH); IR (KBr) ν_{\max} 3462, 3385, 3291, 2955, 2934, 2872, 1742, 1651, 1541, 1497, 1238, 1080 cm⁻¹; HR-MS *m/z* 1140.7150 [M + H]⁺ (calculated for C₅₅H₉₈N₉O₁₆, 1140.7132, Δ = –1.6 ppm). ¹H and ¹³C NMR data are reported in Table 2.

Pseudophomin D (4): white amorphous powder, mp 235.3 °C; [α]_D²⁵ –14.0 (*c* 0.10, MeOH); IR (KBr) ν_{\max} 3337, 2959, 2930, 2870, 1749, 1665, 1541, 1497, 1204, 1070 cm⁻¹; HR-MS *m/z* 1168.7415 [M + H]⁺ (calculated for C₅₇H₁₀₂N₉O₁₆, 1168.7445, Δ = –2.6 ppm). ¹H and ¹³C NMR data are reported in Table 2.

Single-Crystal XRD Analysis. **1** (6.0 mg) was dissolved in 1 mL of MeOH/MeCN/H₂O (5:5:1, *v/v/v*). Colorless transparent crystals of **1** were formed as needle-like shapes by slowly evaporating the solution for 12 h at 28 °C. A suitable crystal (0.15 × 0.12 × 0.11 mm) of **1** was kept at 150.00(10) K for data collection. The crystal data of **1** was processed by Olex2²⁰ and SHELXT,²¹ and the 3D structure of **1** was refined by SHELXL.²²

Crystal data for pseudophomin A (**1**): C₅₅H₉₉N₉O₁₇, *M* = 1158.43 g/mol, orthorhombic, space group *P*2₁2₁2₁ (no. 19), *a* = 14.21040 (10) Å, *b* = 18.7762 (2) Å, *c* = 24.5717 (2) Å, *V* = 6556.15 (10) Å³, *Z* = 4, *T* = 150.00 (10) K, μ (Cu K α) = 0.716 mm⁻¹, *D*_{calc} = 1.174 g/cm³, 31632 reflections measured (5.924° ≤ 2 θ ≤ 143.186°), 12461

unique (*R*_{int} = 0.0314, *R*_{sigma} = 0.0378). The final *R*₁ was 0.0578 (*I* > 2 σ (*I*)) and *wR*₂ was 0.1525 (all data). The details of crystal data and structure refinement for single-crystal XRD analysis of **1** are shown in the Supporting Information.

The X-ray crystallographic data of pseudophomin A (**1**) have been deposited at the Cambridge Crystallographic Data Center (deposition number: CCDC 2207293).

Bioactivity Evaluation of Pseudophomins A–D In Vitro. *P. capsici* (ACCC 37300) was routinely grown on V8 agar (100 mL V8 vegetable juice, 2 g CaCO₃, 20 g agar, per liter) at 25 °C. The antimicrobial activity of pseudophomins against *P. capsici* was evaluated by the paper-disc agar diffusion assay.²³ Purified CLP was adjusted to 1 mg/mL in MeOH, and MeOH was applied as a negative control for testing. Paper discs (diameter = 8 mm) were sterilized before use. Tests for a specific concentration of samples were repeated independently for triplicate.

P. capsici was grown on V8 agar for 5 days at 25 °C. Then, the plates were removed to a laboratory bench for 5 days at room temperature to induce the production of sporangia. Zoospores were released and collected from sporangia by a published protocol.¹⁶ The zoospore suspension was adjusted to approximately 1 × 10⁵ CFU/mL. Pseudophomins A–D were prepared as 50 mM in DMSO first and were further diluted in water to 400 μ M as stock solutions, respectively. A specific amount of the CLP solution was further mixed with the zoospore suspension, to get the final concentrations of CLP in the zoospore solution as 1, 10, and 50 μ M. 10 μ L of the treated zoospore solution was pipetted on a glass slide, and the lysis time (s) of zoospores was directly recorded independently for triplicate under light microscopy.

Assessment of the Biocontrol Activity of Pseudophomins A–D in Plants. Cucumber seeds (jinyan no. 7) were planted in a plastic container (12 × 12 × 12 cm) using a Pindstrup substrate for seedlings (pH = 5.5, The Pindstrup Group). Leaf discs (diameter = 12 mm) were prepared from the second youngest leaves of the 3-week-old cucumber. 1 mL of sterile water was added into each well of 24-well plates, and these leaf discs were floated on the surface of the water in 24-well plates (relative humidity ≥ 90%, 25 °C). A 10 μ L volume of the CLP-treated or control zoospore suspension of *P. capsici* was carefully added dropwise on the top surface of leaf discs. The disease index was calculated as the percentage of the number of spreading lesions on leaf discs versus the total number of leaf discs 72 h postinoculation (hpi). Each experiment was repeated independently in triplicate.

Statistical Analysis. Statistical Package for Social Sciences (SPSS) 26.0 (SPSS Inc., Chicago, USA) was used for statistical analysis of data generated in this study. Mean time(s) for zoospore lysis of *P. capsici* with the same concentration of pseudophomins were compared using Tukey's test (*p* < 0.05). The biocontrol data of *P. capsici* in plants were analyzed by Dunnett's test (*p* < 0.05) by comparing different pseudophomin treatments to the control.

RESULTS

Bioinformatic Characterization of NRPS. 16S rRNA-based phylogeny analysis showed that strain HN8-3 belongs to the *P. fluorescens* subgroup. Further identification of HN8-3

was conducted by a genome-based taxonomy using the Type (Strain) Genome Server (TYGS),²⁴ indicating that HN8-3 is a potential new species. Genome mining of *Pseudomonas* sp. HN8-3 led to the identification of a BGC coding for an NRPS (Figure 1). Phylogeny of adenylation domains from NRPSs of *Pseudomonas* sp. BRG-100 (pseudophomin-producing),²⁵ *P. fluorescens* SBW25 (viscosin-producing),²⁶ *Pseudomonas* sp. COR52 (pseudodesmin-producing), *Pseudomonas* sp. A2W4.9 (viscosinamide-producing),¹³ *Pseudomonas putida* RW10S2 (WLIP-producing),²⁷ *P. lactis* SS101 (massetolide-producing),²⁸ and *Pseudomonas* sp. HN8-3 allowed us to identify a peptide of Leu₁, Glu₂, Thr₃, Ile₄, Leu₅, Ser₆, Leu₇, Ser₈, and Ile₉ from the HN8-3 genome (Figure 1). Condensation (C) domains of NRPSs from these strains were further extracted and are clustered in the Supporting Information. A more detailed inspection of these data has pointed out that adenylation and condensation domains of NRPS from HN8-3 have almost 100% identity with those domains characterized from strain BRG-100, indicating that the CLPs produced by the strain HN8-3 could probably be pseudophomins.

OSMAC Approach. HPLC analysis of crude CLPs produced by HN8-3 in KB broth (Figure 2A) and in MKB

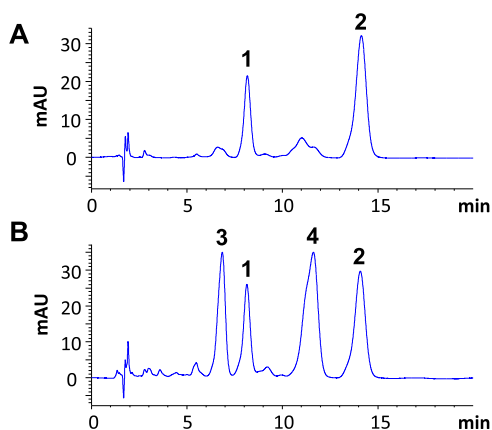
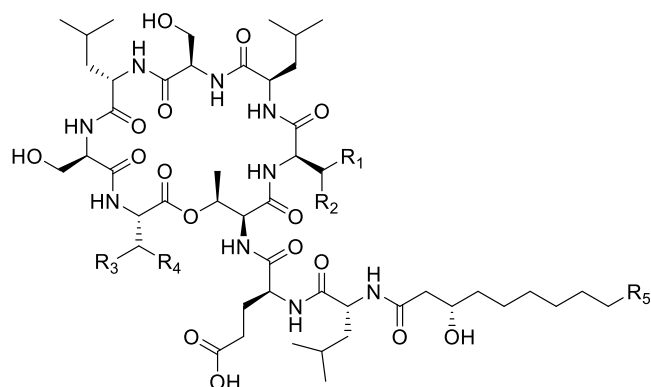


Figure 2. HPLC analysis of crude CLPs from the supernatant of *Pseudomonas* sp. HN8-3 cultured in KB (A) and MKB (B) broths.

broth (Figure 2B) showed distinct metabolic profiles. More specifically, besides **1** ($t_R = 8.2$ min) and **2** ($t_R = 14.1$ min), two additional compounds **3** ($t_R = 6.9$ min) and **4** ($t_R = 11.6$ min) were coproduced by bacterium HN8-3 grown in the MKB broth.

Chemical Identification of CLPs. The ¹H NMR (600 MHz) spectrum of **1** displayed chemical shifts (ppm) for $-\text{CH}_3$ (0.85–1.01), $-\text{CH}_2-$ (1.28), $\text{H}_\alpha/\text{H}_\beta$ (3.71–5.46), and $-\text{NH}-$ (6.96–9.25). These signals are the characteristic signals for amino acids and fatty acid residue. Spin systems of nine amino acids and a fatty acid were recognized from the ¹H–¹H COSY and ¹H–¹H TOCSY spectra of **1**. Amino acids and fatty acids in **1** were further confirmed by ¹H–¹³C HSQC and ¹H–¹³C HMBC experiments. Signals of $-\text{C}=\text{O}-$ in each amino acid were assigned by $J_{1,3}$ correlations (for $-\text{NH}-$ and $-\text{C}=\text{O}-$) observed in the HMBC spectrum. ¹H–¹H ROESY signals of $-\text{NH}-$ in peptide bonds of amino acids established a sequence of Leu₁, Glu₂, Thr₃, Ile₄, Leu₅, Ser₆, Leu₇, Ser₈, and Ile₉ in **1**. A depsi bond formed in C_β of Thr₃, which was confirmed by the unusual chemical shift H_β (5.46) in this amino acid.^{12,13} A correlation of H_β (5.46) in Thr₃ with $-\text{NH}-$ (6.96) in Ile₉ has also confirmed a macrocycle between

Thr₃ and Ile₉ in **1**. A correlation of $\text{CH}_2\alpha$ (2.51) of fatty acid with $-\text{NH}-$ (9.08) of Leu₁ has established the position of fatty acid in **1**. HR-MS data further confirmed a saturated C₁₀ β -hydroxyl fatty acid in **1** (Figure 3). Selected key correlations of



- 1 $\text{R}_1 = \text{CH}_3$ $\text{R}_2 = \text{CH}_2\text{CH}_3$ $\text{R}_3 = \text{CH}_3$ $\text{R}_4 = \text{CH}_2\text{CH}_3$ $\text{R}_5 = \text{CH}_3$
- 2 $\text{R}_1 = \text{CH}_3$ $\text{R}_2 = \text{CH}_2\text{CH}_3$ $\text{R}_3 = \text{CH}_3$ $\text{R}_4 = \text{CH}_2\text{CH}_3$ $\text{R}_5 = \text{CH}_2\text{CH}_2\text{CH}_3$
- 3 $\text{R}_1 = \text{H}$ $\text{R}_2 = \text{CH}(\text{CH}_3)_2$ $\text{R}_3 = \text{H}$ $\text{R}_4 = \text{CH}(\text{CH}_3)_2$ $\text{R}_5 = \text{CH}_3$
- 4 $\text{R}_1 = \text{H}$ $\text{R}_2 = \text{CH}(\text{CH}_3)_2$ $\text{R}_3 = \text{H}$ $\text{R}_4 = \text{CH}(\text{CH}_3)_2$ $\text{R}_5 = \text{CH}_2\text{CH}_2\text{CH}_3$

Figure 3. Chemical structures of **1–4**.

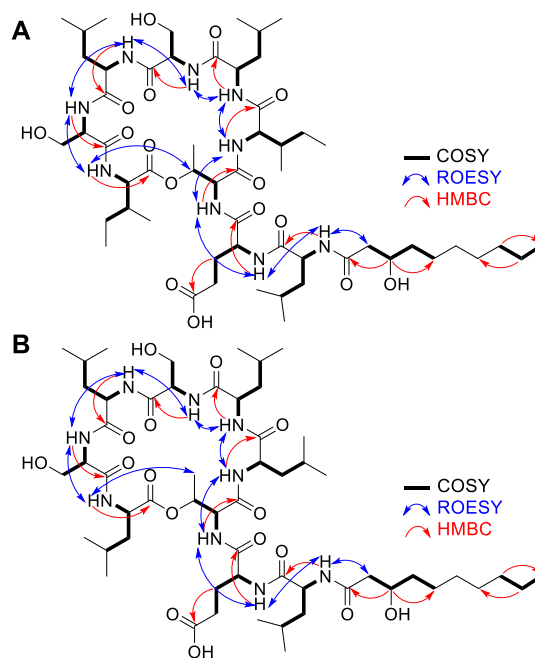


Figure 4. Selected key correlations of 2D NMR spectra for **1** (A) and **3** (B).

2D NMR spectra for **1** are shown in Figure 4. 1D NMR signals of **2** showed almost identical signals with those signals in 1D NMR spectra of **1**, indicating that both compounds shared the same backbone. Collectively, data from HR-MS and 1D NMR have characterized a saturated C₁₂ β -hydroxyl fatty acid moiety in **2**, only differing from **1** at the length of the fatty acid. 1D NMR data of **1** and **2** are assigned in Table 1.

Similarly, HR-MS, 1D NMR, and 2D NMR spectra of **3** have established a sequence of Leu₁, Glu₂, Thr₃, Leu₄, Leu₅,

Ser₆, Leu₇, Ser₈, and Leu₉ linked to a saturated C₁₀ β -hydroxyl fatty acid moiety (Figure 3). A depsi bond was confirmed by the ultrahigh signal of H _{β} (5.51) in Thr₃. A correlation of H _{γ} (1.38) in Thr₃ with $-\text{NH}-$ (7.15) in Leu₉ found in ¹H–¹H ROESY of 3 determined the linkage between the two amino acids. Key correlations from 2D NMR of 3 are shown in Figure 4. 4 showed an identical pattern of NMR spectra with those signals from NMR spectra of 3. HR-MS, 1D NMR, and 2D NMR spectra of 4 confirmed the difference between the two compounds existing in the fatty acid moiety, with a C₁₂ β -hydroxyl fatty acid moiety in 4 (Figure 3). 1D NMR data of 3 and 4 are shown in Table 2.

Absolute Configuration of 1. The refinement of data from single-crystal XRD analysis has determined the configuration of L-Leu₁, D-Glu₂, D-allo-Thr₃, D-Ile₄, D-Leu₅, D-Ser₆, L-Leu₇, D-Ser₈, L-Ile₉, and an R-type C₁₀ β -hydroxyl fatty acid moiety in 1 (Figure 5). Hence, 1 (Figure 3) is

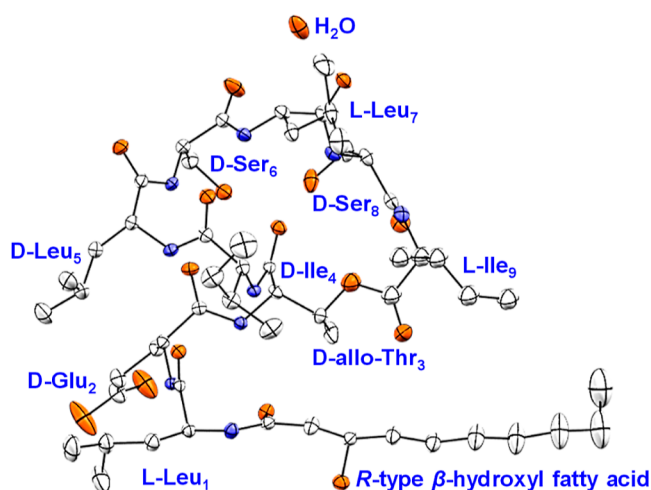


Figure 5. Oakridge thermal ellipsoid plot (ORTEP) diagram of 1. 1 was cocrystallized with one molecule of H₂O, and hydrogens were omitted for clarity.

pseudophomin A.^{29,30} Since 1–4 biosynthetically originate from the same NRPS of *Pseudomonas* sp. HN8-3, it is rational to assign 2–4 to the identical 3D structure as pseudophomin A (1). Taken together, 2 is pseudophomin B;^{29,30} 3 and 4 are two new CLPs dubbed as pseudophomins C and D, respectively (Figure 3).

Biocontrol Activity of Pseudophomins A–D. Antimicrobial tests showed that pseudophomins A–D were inactive to the mycelial growth of *P. capsici*, even though the amount of tested CLPs reached 20 μg /paper disc (data not shown). However, 1, 10, and 50 μM pseudophomins A–D can lyse zoospores of *P. capsici* (Figure 6A), and the capacity of these CLPs in zoospore lysis was positively correlated with their concentrations. Application of 10 or 50 μM pseudophomins A–D-treated zoospores of *P. capsici* on cucumber leaf discs displayed a significant reduction of disease symptoms caused by this pathogen at 72 hpi compared to that of the control (Figure 6B). Moreover, 10 or 50 μM pseudophomins A–D even showed a 100% reduction in the incidence of this pathogen on cucumber leaf discs (Figure 6C).

DISCUSSION

Taxonomic identification of a *Pseudomonas* strain is typically accomplished by the phylogenetic analyses of single or

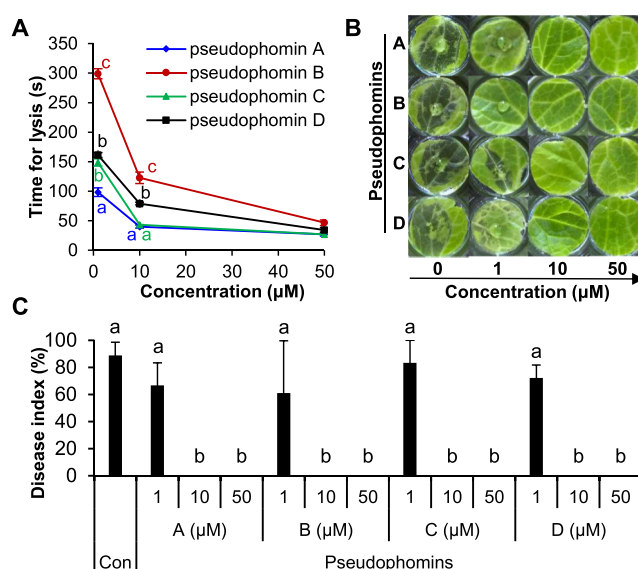


Figure 6. Zoospore lysis of pseudophomins A–D (A), typical disease symptoms of pseudophomins A–D-treated zoospores of *P. capsici* on cucumber leaf discs from a representative experiment (B) and biocontrol data of pseudophomins A–D against zoospores of *P. capsici* in plants (C). Different lowercase letters indicate significant differences among treatments ($p < 0.05$). Con = control.

multilocus housekeeping genes. The housekeeping genes used for the taxonomic study of *Pseudomonas* spp. are typically 16S rRNA, rpoD, and so forth.¹⁷ In the current study, a 16S rRNA gene-based phylogenetic tree indicated that the strain HN8-3 is a potential new *Pseudomonas* species. However, comparison of the genome of a potential new microbe with other well-established type strains is a promising strategy for the taxonomic characterization of new strains. Here, we further used TYGS, a well-developed database and web server for the identification of microbes, to complete the taxonomy of the strain HN8-3. Data from TYGS have confirmed that the strain HN8-3 is a new species, which needs to be identified elsewhere in detail in future.

Supplementing exogenous amino acids in the cultural substrate as an OSMAC strategy has been used previously for the production of CLP surfactin variants from *Bacillus* spp.^{31–34} An OSMAC protocol involving supplementing L-Leu in KB broth has resulted in the production and characterization of new CLPs pseudophomins C (3) and D (4) from *Pseudomonas* sp. HN8-3, while pseudophomins A (1) and B (2) could be coproduced in the same medium (Figure 2). However, addition of other amino acids (such as D-Leu, L-Val, D-Val, L-Ile, and D-Ile) in KB broth was inactive to stimulate extra CLPs from *Pseudomonas* sp. HN8-3 by HPLC analysis (data not shown). NMR analyses showed that pseudophomins C and D are Leu-rich CLPs compared to the structures of pseudophomins A and B (Figure 3). However, the mechanisms underpinning such phenomena are not clear and still need to be elucidated in further studies.

It is proposed that similar OSMAC approaches (namely, supplementing proteinaceous amino acids in a basal medium) could be applied to other CLP-producing *Pseudomonas* spp. We have applied a similar OSMAC approach (by adding L-Val, L-Ile, and L-Leu in KB broth) for an MDN-0066-producing *Pseudomonas moraviensis* HN2,³⁵ a WLIP-producing *Pseudomonas* sp. Q3-1 (Ma Z., unpublished data), and a viscosin-

producing *Pseudomonas* sp. HN11 (Ma Z., unpublished data); in these cases, they all produce additional peak(s) of CLPs in the MKB broth compared to that of metabolic profiles in the KB broth. To sum up, future studies should be focused on re-evaluating the metabolic profiles of various NRPSs in *Pseudomonas* spp. using this type of OSMAC strategy, which will probably lead to the production of new variants of peptidic compounds.

A set of well-developed methods, such as C₃ and 2D C₃ Marfey's method,³⁶ (C–H) α NMR fingerprint matching approach,³⁷ Mosher's method,³⁸ chemical synthesis,³⁹ and bioinformatic analyses⁴⁰ could be tentatively applied for the elucidation of the 3D structure of bacterial CLPs. However, some CLPs are composed of several same amino acids with different configurations (L/D) (for instance 2 \times L-Leu, 1 \times D-Leu, 1 \times L-Ile, and 1 \times D-Ile in pseudophomin A, Figure 3); in such conditions, it will remain a challenge in practice to precisely assign these amino acids in the correct position. Single-crystal XRD is widely applied to circumvent this problem. The 3D structure of pseudophomins A and B was determined previously by chemical degradation and single-crystal XRD analysis.^{29,30} Likewise, the 3D structure of pseudophomin A (1) was characterized by single-crystal XRD analysis in the current study (Figure 5). However, instead of using dichloromethane/MeOH (1:9, v/v) for crystal growth of pseudophomin A,³⁰ an alternative solvent MeOH/MeCN/H₂O (5:5:1, v/v/v) was applied for the crystallization in this study. It is worth mentioning that for these CLPs cannot form suitable crystals for XRD analyses; a combinational use of two or more of the abovementioned methods will probably be a solution.

The mode of action of other biocontrol agents (such as *Streptomyces*, *Pseudomonas*, *Burkholderia*, *Flavobacterium*, and *Bacillus* spp.) on *P. capsici* included inhibition of mycelial growth,^{41,42} suppression of sporangium formation and zoosporogenesis,^{42,43} inhibition of germination on zoospores,^{42–44} and lysis of zoospores.^{16,44} The active secondary metabolites from these biocontrol strains directly contributing to the biocontrol of *P. capsici* are 1H-pyrrole-2-carboxylic acid,⁴¹ a volatile compound (2,4-di-*tert*-butylphenol)⁴² and CLPs putisolvin,¹⁶ surfactin, and fengycin.⁴⁴ Moreover, we have shown in this study that CLPs pseudophomins A–D (1–4) are capable of decreasing the incidence of disease symptoms caused by *P. capsici* on cucumber leaf discs via the lysis of zoospores of this pathogen (Figure 6). Additionally, the herbicidal (such as *Setaria viridis*) and antifungal (such as *Rhizoctonia solani*, *Sclerotinia sclerotiorum*, *Alternaria brassicae*, and *Phoma lingam*) activities of pseudophomins A and B have been reported previously.²⁹ Collectively, these data could provide clues for developing pseudophomins as potential biopesticides to be used in agricultural practices. However, to gain more insights into the biocontrol potential of pseudophomins, the antagonistic activity of these CLPs against other *Phytophthora* pathogens (such as *Phytophthora infestans*, the causal agent of potato late blight) should be studied further.

ASSOCIATED CONTENT

Supporting Information

The Supporting Information is available free of charge at <https://pubs.acs.org/doi/10.1021/acs.jafc.3c00137>.

16S rRNA-based neighbor-joining tree of *Pseudomonas* sp. HN8-3; neighbor-joining tree of adenylation and condensation domains from NRPSs in selected *Pseudomonas* spp.; HR-MS, UV, and IR spectra of 1–4; ¹H NMR, ¹³C NMR, ¹H–¹H COSY, ¹H–¹³C HSQC, ¹H–¹³C HMBC, and ¹H–¹H ROESY spectra of 1, 3, and 4; and ¹H and ¹³C NMR spectra of 2 (PDF)

Structural refinement of the crystal of 1 and crystallographic data of 1 (CIF)

AUTHOR INFORMATION

Corresponding Author

Zongwang Ma – College of Life Science, Northwest Normal University, 730070 Lanzhou, China; orcid.org/0000-0002-6123-1529; Email: zongwang.ma@nwnu.edu.cn

Author

Jun Sheng – College of Life Science, Northwest Normal University, 730070 Lanzhou, China

Complete contact information is available at: <https://pubs.acs.org/10.1021/acs.jafc.3c00137>

Author Contributions

Z.M. conceived and designed the study. J.S. conducted the in vitro bioassays of pseudophomins A–D and was partially involved in the plant assays of pseudophomins A–D. Z.M. performed the rest of the experiments, analyzed the data, and wrote the manuscript. Both authors have approved the manuscript for submission.

Funding

This study was supported by grants from the National Natural Science Foundation of China (no. 32060625) and the Natural Science Foundation of Gansu Province (no. 20JR5RA527).

Notes

The authors declare no competing financial interest.

ACKNOWLEDGMENTS

The authors thank Haishan Wang for testing the physical–chemical properties of pseudophomins A–D and for performing single-crystal XRD analysis and structural refinement of pseudophomin A. The Agricultural Culture Collection of China (ACCC) is acknowledged by the authors for providing *Phytophthora capsici*.

REFERENCES

- (1) Kamoun, S.; Furzer, O.; Jones, J. D. G.; Judelson, H. S.; Ali, G. S.; Dalio, R. J. D.; Roy, S. G.; Schena, L.; Zambounis, A.; Panabières, F.; Cahill, D.; Ruocco, M.; Figueiredo, A.; Chen, X. R.; Hulvey, J.; Stam, R.; Lamour, K.; Gijzen, M.; Tyler, B. M.; Grünwald, N. J.; Mukhtar, M. S.; Tomé, D. F. A.; Tör, M.; Van Den Ackerveken, G.; McDowell, J.; Daayf, F.; Fry, W. E.; Lindqvist-Kreuzer, H.; Meijer, H. J. G.; Petre, B.; Ristaino, J.; Yoshida, K.; Birch, P. R. J.; Govers, F. The Top 10 oomycete pathogens in molecular plant pathology. *Mol. Plant Pathol.* **2015**, *16*, 413–434.
- (2) Lamour, K. H.; Stam, R.; Jupe, J.; Huitema, E. The oomycete broad-host-range pathogen *Phytophthora capsici*. *Mol. Plant Pathol.* **2012**, *13*, 329–337.
- (3) Velivelli, S. L. S.; De Vos, P.; Kromann, P.; Declerck, S.; Prestwich, B. D. Biological control agents: from field to market, problems, and challenges. *Trends Biotechnol.* **2014**, *32*, 493–496.
- (4) Oni, F. E.; Esmaeel, Q.; Onyeka, J. T.; Adeleke, R.; Jacquard, C.; Clement, C.; Gross, H.; Ait Barka, E.; Höfte, M. *Pseudomonas*

- lipopeptide-mediated biocontrol: chemotaxonomy and biological activity. *Molecules* **2022**, *27*, 372.
- (5) Girard, L.; Lood, C.; Höfte, M.; Vandamme, P.; Rokni-Zadeh, H.; van Noort, V.; Lavigne, R.; De Mot, R. The ever-expanding *Pseudomonas* genus: description of 43 new species and partition of the *Pseudomonas putida* group. *Microorganisms* **2021**, *9*, 1766.
- (6) Gross, H.; Loper, J. E. Genomics of secondary metabolite production by *Pseudomonas* spp. *Nat. Prod. Rep.* **2009**, *26*, 1408–1446.
- (7) Pršić, J.; Ongena, M. Elicitors of plant immunity triggered by beneficial bacteria. *Front. Plant Sci.* **2020**, *11*, 594530.
- (8) Oni, F. E.; Geudens, N.; Omoboye, O. O.; Bertier, L.; Hua, H. G. K.; Adiobo, A.; Sinnaeve, D.; Martins, J. C.; Höfte, M. Fluorescent *Pseudomonas* and cyclic lipopeptide diversity in the rhizosphere of cocoyam (*Xanthosoma sagittifolium*). *Environ. Microbiol.* **2019**, *21*, 1019–1034.
- (9) Götze, S.; Stallforth, P. Structure, properties, and biological functions of nonribosomal lipopeptides from pseudomonads. *Nat. Prod. Rep.* **2020**, *37*, 29–54.
- (10) Süßmuth, R. D.; Mainz, A. Nonribosomal peptide synthesis-principles and prospects. *Angew. Chem., Int. Ed. Engl.* **2017**, *56*, 3770–3821.
- (11) Blin, K.; Shaw, S.; Kloosterman, A. M.; Charlop-Powers, Z.; van Wezel, G. P.; Medema, M. H.; Weber, T. antiSMASH 6.0: improving cluster detection and comparison capabilities. *Nucleic Acids Res.* **2021**, *49*, W29–W35.
- (12) Omoboye, O. O.; Geudens, N.; Duban, M.; Chevalier, M.; Flahaut, C.; Martins, J. C.; Leclère, V.; Oni, F. E.; Höfte, M.; Höfte, M. *Pseudomonas* sp. COW3 produces new bananamide-type cyclic lipopeptides with antimicrobial activity against *Pythium myriotylum* and *Pyricularia oryzae*. *Molecules* **2019**, *24*, 4170.
- (13) Oni, F. E.; Geudens, N.; Adiobo, A.; Omoboye, O. O.; Enow, E. A.; Onyeka, J. T.; Salami, A. E.; De Mot, R.; Martins, J. C.; Höfte, M. Biosynthesis and antimicrobial activity of pseudodesmin and viscosinamide cyclic lipopeptides produced by *Pseudomonas* associated with the cocoyam rhizosphere. *Microorganisms* **2020**, *8*, 1079.
- (14) Oni, F. E.; Geudens, N.; Onyeka, J. T.; Olorunleke, O. F.; Salami, A. E.; Omoboye, O. O.; Arias, A. A.; Adiobo, A.; De Neve, S.; Ongena, M.; Martins, J. C.; Höfte, M. Cyclic lipopeptide-producing *Pseudomonas koreensis* group strains dominate the cocoyam rhizosphere of a *Pythium* root rot suppressive soil contrasting with *P. putida* prominence in conducive soils. *Environ. Microbiol.* **2020**, *22*, 5137–5155.
- (15) Zhou, L.; de Jong, A.; Yi, Y.; Kuipers, O. P. Identification, isolation, and characterization of medipeptins, antimicrobial peptides from *Pseudomonas mediterranea* EDOX. *Front. Microbiol.* **2021**, *12*, 732771.
- (16) Kruijff, M.; Tran, H.; Raaijmakers, J. M. Functional, genetic and chemical characterization of biosurfactants produced by plant growth-promoting *Pseudomonas putida* 267. *J. Appl. Microbiol.* **2009**, *107*, 546–556.
- (17) Lopes, L. D.; Davis, E. W.; Pereira e Silva, M. d. C.; Weisberg, A. J.; Bresciani, L.; Chang, J. H.; Loper, J. E.; Andreote, F. D.; Andreote, F. D. Tropical soils are a reservoir for fluorescent *Pseudomonas* spp. biodiversity. *Environ. Microbiol.* **2018**, *20*, 62–74.
- (18) Ma, Z. Analysis of the complete genome sequence of a rhizosphere-derived *Pseudomonas* sp. HN3-2 leads to the characterization of a cyclic lipopeptide-type antibiotic bananamide C. *3 Biotech* **2022**, *12*, 35.
- (19) Tamura, K.; Stecher, G.; Peterson, D.; Filipowski, A.; Kumar, S. MEGA6: molecular evolutionary genetics analysis version 6.0. *Mol. Biol. Evol.* **2013**, *30*, 2725–2729.
- (20) Dolomanov, O. V.; Bourhis, L. J.; Gildea, R. J.; Howard, J. A. K.; Puschmann, H. OLEX2: a complete structure solution, refinement and analysis program. *J. Appl. Crystallogr.* **2009**, *42*, 339–341.
- (21) Sheldrick, G. M. SHELXT-Integrated space-group and crystal-structure determination. *Acta Crystallogr., Sect. A: Found. Adv.* **2015**, *71*, 3–8.
- (22) Sheldrick, G. M. Crystal structure refinement with SHELXL. *Acta Crystallogr., Sect. C: Struct. Chem.* **2015**, *71*, 3–8.
- (23) Ma, Z.; Wang, N.; Hu, J.; Wang, S. Isolation and characterization of a new iturinic lipopeptide, mojavensin A produced by a marine-derived bacterium *Bacillus mojavensis* B0621A. *J. Antibiot.* **2012**, *65*, 317–322.
- (24) Meier-Kolthoff, J. P.; Göker, M. TYGS is an automated high-throughput platform for state-of-the-art genome-based taxonomy. *Nat. Commun.* **2019**, *10*, 2182.
- (25) Dumonceaux, T. J.; Town, J.; Links, M. G.; Boyetchko, S. High-quality draft genome sequence of *Pseudomonas* sp. BRG100, a strain with bioherbicidal properties against *Setaria viridis* (Green Foxtail) and other pests of agricultural significance. *Genome Announc.* **2014**, *2*, No. e00995.
- (26) De Bruijn, I.; de Kock, M. J. D.; Yang, M.; de Waard, P.; van Beek, T. A.; Raaijmakers, J. M. Genome-based discovery, structure prediction and functional analysis of cyclic lipopeptide antibiotics in *Pseudomonas* species. *Mol. Microbiol.* **2007**, *63*, 417–428.
- (27) Rokni-Zadeh, H.; Li, W.; Sanchez-Rodriguez, A.; Sinnaeve, D.; Rozenski, J.; Martins, J. C.; De Mot, R. Genetic and functional characterization of cyclic lipopeptide white-line-inducing principle (WLIP) production by rice rhizosphere isolate *Pseudomonas putida* RW10S2. *Appl. Environ. Microbiol.* **2012**, *78*, 4826–4834.
- (28) De Bruijn, I.; de Kock, M. J. D.; de Waard, P.; van Beek, T. A.; Raaijmakers, J. M. Massetolide A biosynthesis in *Pseudomonas fluorescens*. *J. Bacteriol.* **2008**, *190*, 2777–2789.
- (29) Pedras, M. S.; Ismail, N.; Quail, J. W.; Boyetchko, S. M. Structure, chemistry, and biological activity of pseudophomins A and B, new cyclic lipopeptides isolated from the biocontrol bacterium *Pseudomonas fluorescens*. *Phytochemistry* **2003**, *34*, 1105–1114.
- (30) Quail, J. W.; Ismail, N.; Pedras, M. S.; Boyetchko, S. M. Pseudophomins A and B, a class of cyclic lipopeptides isolated from a *Pseudomonas* species. *Acta Crystallogr., Sect. C: Cryst. Struct. Commun.* **2002**, *58*, o268–o271.
- (31) Menkhous, M.; Ullrich, C.; Kluge, B.; Vater, J.; Vollenbroich, D.; Kamp, R. M. Structural and functional organization of the surfactin synthetase multienzyme system. *J. Biol. Chem.* **1993**, *268*, 7678–7684.
- (32) Peypoux, F.; Bonmatin, J.; Labbe, H.; Grangemard, I.; Das, B. C.; Ptak, M.; Wallach, J.; Michel, G. [Ala4]Surfactin, a novel isoform from *Bacillus subtilis* studied by mass and NMR spectroscopies. *Eur. J. Biochem.* **1994**, *224*, 89–96.
- (33) Grangemard, I.; Peypoux, F.; Wallach, J.; Das, B. C.; Labbé, H.; Caille, A.; Genest, M.; Maget-Dana, R.; Ptak, M.; Bonmatin, J. M. Lipopeptides with improved properties: structure by NMR, purification by HPLC and structure-activity relationships of new isoleucyl-rich surfactins. *J. Pept. Sci.* **1997**, *3*, 145–154.
- (34) Ma, Z.; Zhang, S.; Zhang, S.; Wu, G.; Shao, Y.; Mi, Q.; Liang, J.; Sun, K.; Hu, J. Isolation and characterization of a new cyclic lipopeptide surfactin from a marine-derived *Bacillus velezensis* SH-B74. *J. Antibiot.* **2020**, *73*, 863–867.
- (35) Ma, Z. Genome mining and chemical characterization of a new cyclic lipopeptide associated with MDN-0066 from *Pseudomonas moraviensis* HN2 cultured in a valine-rich medium. *J. Antibiot.* **2023**, *76*, 244–248.
- (36) Vijayarathay, S.; Prasad, P.; Fremlin, L. J.; Ratnayake, R.; Salim, A. A.; Khalil, Z.; Capon, R. J. C₃ and 2D C₃ Marfey's methods for amino acid analysis in natural products. *J. Nat. Prod.* **2016**, *79*, 421–427.
- (37) De Roo, V.; Verleysen, Y.; Kovács, B.; De Vleeschouwer, M.; Muangkaew, P.; Girard, L.; Höfte, M.; De Mot, R.; Madder, A.; Geudens, N.; Martins, J. C. An nuclear magnetic resonance fingerprint matching approach for the identification and structural re-evaluation of *Pseudomonas* Lipopeptides. *Microbiol. Spectrum* **2022**, *10*, No. e0126122.
- (38) Tanaka, K.; Amaki, Y.; Ishihara, A.; Nakajima, H. Synergistic effects of [Ile-]surfactin homologues with bacillomycin D in

suppression of gray mold disease by *Bacillus amyloliquefaciens* biocontrol strain SD-32. *J. Agric. Food Chem.* **2015**, *63*, 5344–5353.

(39) Bando, Y.; Hou, Y.; Seyfarth, L.; Probst, J.; Götze, S.; Bogacz, M.; Hellmich, U. A.; Stallforth, P.; Mittag, M.; Arndt, H. D. Total synthesis and structure correction of the cyclic lipopeptide orfamide A. *Chemistry* **2022**, *28*, No. e202104417.

(40) Jahanshah, G.; Yan, Q.; Gerhardt, H.; Pataj, Z.; Lämmerhofer, M.; Pianet, I.; Josten, M.; Sahl, H. G.; Silby, M. W.; Loper, J. E.; Gross, H. Discovery of the cyclic lipopeptide gacamide A by genome mining and repair of the defective GacA regulator in *Pseudomonas fluorescens* Pf0-1. *J. Nat. Prod.* **2019**, *82*, 301–308.

(41) He, H.; Hao, X.; Zhou, W.; Shi, N.; Feng, J.; Han, L. Identification of antimicrobial metabolites produced by a potential biocontrol Actinomycete strain A217. *J. Appl. Microbiol.* **2020**, *128*, 1143–1152.

(42) Sang, M. K.; Kim, K. D. The volatile-producing *Flavobacterium johnsoniae* strain GSE09 shows biocontrol activity against *Phytophthora capsici* in pepper. *J. Appl. Microbiol.* **2012**, *113*, 383–398.

(43) Khatun, A.; Farhana, T.; Sabir, A. A.; Islam, S. M. N.; West, H. M.; Rahman, M.; Islam, T. *Pseudomonas* and *Burkholderia* inhibit growth and asexual development of *Phytophthora capsici*. *Z. Naturforsch., C: J. Biosci.* **2018**, *73*, 123–135.

(44) Ley-López, N.; Basilio Heredia, J.; San Martín-Hernández, C.; Ibarra-Rodríguez, J. R.; Angulo-Escalante, M. Á.; García-Estrada, R. S. Induced biosynthesis of fengycin and surfactin in a strain of *Bacillus amyloliquefaciens* with oomycetocidal activity on zoospores of *Phytophthora capsici*. *Rev. Argent. Microbiol.* **2022**, *54*, 181–191.